

# **ADS4100**

## **Intrepid Geophysics Internship**



Isaac Wood

# Contents

<b>Executive Summary.....</b>	<b>2</b>
<b>Introduction.....</b>	<b>3</b>
Intrepid Geophysics.....	3
Gravitational Data.....	3
Inversion.....	4
Machine Learning.....	4
Project.....	5
<b>Literature Review.....</b>	<b>5</b>
<b>Data.....</b>	<b>9</b>
Synthetic Data.....	9
<b>Research.....</b>	<b>13</b>
Synthetic Model Generation.....	13
Gravitational Acceleration.....	16
Machine Learning.....	16
Realistic Data Testing.....	18
<b>Results.....</b>	<b>20</b>
Curriculum Training.....	20
Synthetic Data.....	21
Realistic Data.....	24
<b>Conclusion.....</b>	<b>27</b>
<b>References.....</b>	<b>29</b>

## Executive Summary

Understanding subsurface geological structures is critical for resource exploration and infrastructure assessment. Traditionally, this understanding is gained through extensive drilling and excavation to get samples of the structure however this is resource and time intensive as well as potentially dangerous. Using measurements of gravitational acceleration at the surface, which are comparatively easy to collect, a process called inversion can be applied to develop an image of what the three dimensional subsurface looks like based on that two dimensional gravitational acceleration data.

However, traditional methods of gravity inversion are limited by the inherent non-uniqueness of the problem, any one gravitational acceleration measurement could have infinite possible density solutions. The use of machine learning in this field has been explored to capture this complex relationship, but due to the lack of real training data has relied extensively on simple synthetic models to train their neural networks. This project, undertaken during an internship at Intrepid Geophysics, explored how more realistic synthetic training data can enhance this machine learning inversion process. More specifically, this project aimed to find a method to generate synthetic geomodels that more accurately mimic real-world complexity by incorporating realistic geophysical prior information. The corresponding gravitational acceleration responses at the surface of these models were then to be calculated and used as an input for training a neural network model to effectively perform inversion. This was then to be finally authenticated using more realistic, professionally developed testing data.

Utilising open-source python software StructuralGeo, five datasets were created of synthetic models simulating various faulted and intrusive features. Accompanying each of these synthetic density models was the corresponding gravitational acceleration at the surface calculated using forward modelling equations in PyTreeGrav, another open-source python software. Taking advantage of a more human, curriculum training approach to identify simpler features before more challenging ones, a convolutional neural network with a U-Net structure was implemented. This network was trained to learn the complex relationship between the input gravitational data and the complex subsurface densities, before being validated with unseen synthetic data and tested finally on much more realistic data developed by experienced geophysicists.

The model was able to successfully recreate the major subsurface density patterns of the synthetic training data, achieving a testing L1 loss of 0.0230 and an R<sup>2</sup> score of 0.9067 after being trained on the full collection of data. This accuracy is reinforced by a visual inspection of the final predictions showing the accurate estimation of feature locations even in the more complex mixed feature designs. When applied to the more realistic 2014 SEAM dataset, representing an authentically designed salt body, the trained network was able to reproduce large-scale features and some of the changing aspects of the structure, however it struggled with accurate scaling of the density values and a loss of accuracy at increased depths. This work highlights the potential applications of machine learning in critical resource exploration while demonstrating the use of realistic synthetic data in model training. Moving forward, with more authentic data the model could be fine-tuned to solve scaling issues when applied to data in the field as well as further developed in conjunction with professional geophysicists to improve training data. Overall, the pipeline that was developed for synthetic data generation,

machine learning and authentic data testing provides insight and a launching point for further research into machine learning for geophysical inversion.

## Introduction

### Intrepid Geophysics

Intrepid Geophysics is a Melbourne based geoscientific software company that specialises in developing products for advanced geological modelling, data integration and inversion. Their suite of products, which includes Intrepid and GeoModeller, is used globally for subsurface interpretation and resource exploration. Additionally, they also deliver consulting services across the geophysics industry and have been providing “potential field geophysics and integrated geology for more than 35 years” (Intrepid Geophysics, 2021). Operating at the intersection of commercial software development and applied geoscientific research, Intrepid’s tools are employed globally by geological surveys, mining and petroleum companies as well academic and governmental institutions.

One of the key services provided by the Intrepid software and through their consulting services is inversion. Inversion describes the process of using the observed geophysical measurements, like gravitational acceleration, around a certain area to try and predict the geological structures in that same area. With effective and accurate inversion we can obtain crucial insights into geological structures and the potential resources which would have been otherwise unknown, which is why “gravity prospecting is one of the most traditional and extensively used geophysical prospecting methods” (M Lv et al., 2023).

### Gravitational Data

The process of gravity inversion begins with accurate gravitational acceleration data. Sourced in a variety of ways, a common method is through the use of Airborne Geophysical Surveys. These surveys utilise highly sensitive instruments on specially equipped aircraft which, when flown in parallel lines, provide a rapid method to map fine variations in gravitational acceleration over a specific area (M.B. Aminu et al., 2024). This can result when visualised, in a heat map of different gravitational strengths (Figure 1). These gravitational differences are traditionally measured in units of mGals which are incredibly subtle variations in the downward pull, indiscernible to the human body but detectable to the instruments deployed on these surveys.

These differences in gravitational acceleration stem significantly from the topographical distinctions across the area, if the survey flies over a large hill then there is more mass directly underneath resulting in a stronger gravitational pull, however topographical deviations can be corrected for. Once they have been corrected the survey is essentially

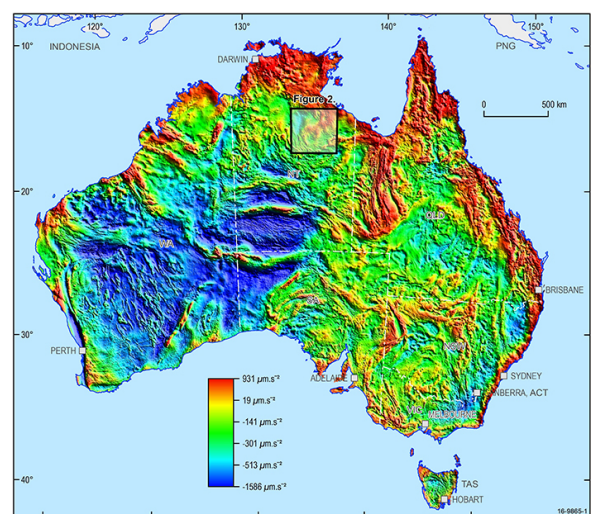


Fig. 1 Variation of gravitational acceleration mapped across Australia (Geoscience Australia, 2016).

measuring over a flat plane and the variations in gravitational acceleration strength now originate in the changing densities and formations in the geological subsurface (Nozaki, 2006).

## Inversion

Traditionally, understanding the subsurface structure of the Earth require extensive drilling, excavation and geological expertise but these processes take time, resources and incur significant risks in their undertaking. The collection of gravitational data however, is comparatively easy so if gravitational data can be used to directly predict what is underground it can streamline the exploration process reducing cost and risk. In an ideal world it would be possible to go from two dimensional gravity measurement straight to three dimensional subsurface reconstruction but difficulties arise in the classical methods of approaching this problem. Classical inversion methods often rely on iterative forward modelling, this means that a subsurface density model is initialised based on some prior geological information and then adjusted until its calculated gravitational response matches the observed surface data. These methods can be robust but tend to be computationally intensive and highly sensitive to noise and prior assumptions. Another of the challenges with this method for geophysical prediction lies in the non-uniqueness of the defined problem (Wu et al., 2023). This is due to the fact that multiple geological formations under the surface could create the same gravitational measurement above. Different layers on top of one another, the insertion of a new rock type into the formation or an extending depth of one layer could all produce identical surface gravitational responses. Essentially, every gravitational acceleration mapping has infinite possible subsurface density solutions, which is why gravity inversion has been such a longstanding field of work in geophysics and has led to the introduction of more modern machine learning techniques for exploration of this field.

## Machine Learning

Recently, there has been increased interest in the application of machine learning techniques to the problem of gravity inversion. Contrasting to historical numerical methods utilising classical physical equations, machine learning and neural networks can adapt and learn complex non-linear mappings to ideally produce more accurate and efficient results. However such networks require extensive amounts of information to train and learn relationships from before they can be realistically used in genuine applications. This requirement means that machine learning models in geophysics often rely on synthetic datasets for training due to the limited availability of high-quality labelled field data, as it requires extensive resources and experience to acquire (Garayt et al., 2025). However, many current synthetic models oversimplify geological structures and geophysical responses, leading to models that do not generalise well to real-world scenarios. These models depict subsurface geological features as simple prisms and are lacking the intricacies of key features such as faults and insertions which are inherent to true geological structures.

## **Project**

This project aims to find a method to generate synthetic geological models that more accurately mimic real-world complexity through the incorporation of realistic geological and geophysical prior information, as well as data-driven realism constraints. The corresponding gravity responses of these models are then to be calculated to evaluate the use of these synthetic models for downstream geological machine learning tasks like anomaly detection and gravity inversion. Through the implementation of StructuralGeo, an open-source geological generation program, as well as PyTreeGrav for the gravitational data synthesis this project also aims to establish a reproducible workflow for the Intrepid Geophysics environment and validate the use of machine learning in geophysical inversion.

## **Literature Review**

The inversion of gravity has long been a fundamental technique in geophysics for the estimation of subsurface geological formations from observed gravity data. However, traditional physics based approaches face persistent challenges in the non-uniqueness, noise-sensitivity and limited accuracy nature of observations (Blakely, 1995). More modern machine learning models in geophysics often depend on synthetic datasets for training, as high-quality labelled field data is scarce. However, many existing synthetic models simplify geological structures and geophysical responses, limiting their ability to generalize to real-world conditions.

Mining has always played a significant role in the Australian economy, from 19th century gold rushes through to the current day (Hajkowicz et al., 2011). The collection of resources provides the grounding point for economic growth. According to the Minerals Council of Australia, 'In 2021-22, Australia's exports of minerals, metals and energy commodities was worth \$413 billion and accounted for 69 per cent of total export revenue.' An important aspect of this revenue is in the contribution of 'bauxite, copper, nickel, lithium,' which are critical for the global transition to net zero emissions. With more accurate mineral and subsurface structure prediction the efficiency of resource collection could be improved, driving sustainable resource management and advancing our scientific understanding of Earth's evolutionary history.

Challenging the accepted theory that the velocity of a freely falling body is proportional to its weight, in 1604 Galileo came to the realisation that gravity acts at a constant rate on all objects. This has since resulted in the collection of gravitational information expanding to obtain increased accuracies less than 1 milligal precisions ( $0.00001 \text{ ms}^{-2}$ ) (N et al., 2005). This increasingly accurate data thus allowed for the application of the focus of this report, gravity inversion. One of the first successful applications of geological structure prediction came when Manik Talwani developed, as part of a dissertation, a method for calculating the 2D gravity anomaly due to a polygon in a vertical cross-section (Talwani et al., 1959). This was one of the first studies to successfully gather gravitational information gravity measurements at sea.

Ultimately, with increased computing power, this developed into a three dimensional approach to address the ‘inherent nonuniqueness that exists in any geophysical method based upon a static potential field’ (Li & Oldenburg, 1998). Li & Oldenburg introduced a 3D inversion method with depth weighting to stabilise the solution, making large 3D problems computationally feasible. While these papers mark landmark improvements, the fact remains that the inversion of gravity data is ‘usually ill-posed and the result is inherently non-unique. For the same gravity anomaly, infinite mathematical solutions can be found’ (Li et al., 2023). This results in a significant reliance on prior information and background knowledge to fine tune the final model selection.

Understanding what lies beneath the surface of the earth has been a longstanding challenge in geomodelling. The earliest efforts of exploration were based on surface observations, of things such as rocky outcrops, and a reliance on the intuition of experts (Wigley, 2016). This was then developed upon, as the field matured, to include informational sources such as boreholes which can describe the subsurface conditions. ‘The central problem of characterizing significant rock and fluid properties in the subsurface is that, to date, there is no inexpensive and comprehensive way to directly measure these properties’ (Wellmann, 2022). This lack of detailed field data leads to difficulties in the application of machine learning for geophysics applications. Attempts have been made to use synthetic datasets to supplement this lack of authentic data for training these models however, ‘synthetic datasets often do not capture the reality of the field/real experiment, and we end up with poor performance of the trained neural network’ (Alkhailifah et al., 2021). There is a clear need for more accurate synthetic data that can be utilised in machine learning.

Recently, with a rapid development in computational performance and increased attention in general machine learning frameworks, deep learning methods have been at the forefront of improvement in gravity inversion research. Most prevalently applied in research is the convolutional neural network architecture (CNNs). A 2023 paper from Li et al. implements GV-Net, a CNN trained on synthetic gravity data in the form of varying density prisms in a certain area (Fig. 2). This results in relatively accurate predictions of simple bodies based on their gravity readings. Similarly, a 2024 paper by Zhou et al., 2024 utilises the CNN architecture in a U-Net design to encode the two dimensional gravity data, extract the key features and then decode to expand the channels for a three dimensional density representation. Trained comparably on random density prisms, this model shows success in its predictions on basic training data as well as some reliable representation of areas under the Gonghe Basin (Zhou et al., 2024). While promising, in their presented accuracy and visual inspections, these papers both depict a

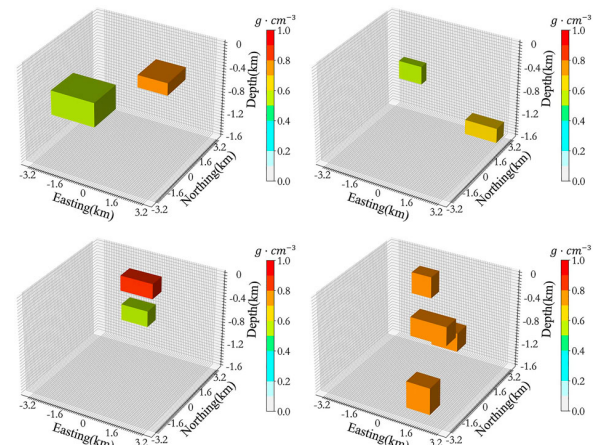


Fig. 2 Examples of the random density models used for model training (Li et al., 2023)

continued lack of realism in their synthetic training data, failing to capture the complexities of subsurface geometries. This results in predictions, while being representative of their training data and able to locate potential anomalies, they are unable to capture true geophysical structures that are sought after in mineral exploration. This reemphasises the requirement for more realistic synthetic datasets to fill the gap in authentic training data.

'Visualizing the first few kilometers of the Earth's subsurface, a long-standing challenge gating a virtually inexhaustible list of important applications, is coming within reach through deep learning' (Ghyselincks et al., 2025). A 2022 study approaches the inherent lack of available data through the implementation of a 'generator of 2D subsurface models based on deep generative adversarial networks' (Vladimir Puzyrev et al., 2022). In recent years the task of creating synthetic data has been the subject of increasing research with Generative Adversarial Networks (GANs) proving to have become, 'One of the most important developments in machine learning and computer vision in the 2010s' (Vladimir Puzyrev et al., 2022). These models consist of two parts: a generator, which learns from real data to try and generate fake data which is indistinguishable, and a discriminator which determines whether the generated data is realistic. When used in combination these two elements learn from each other resulting in continuous improvement until an equilibrium is reached (Salehi et al., 2020). In the geophysical context this process has been applied to generate realistic 2D subsurface models in combination with the open source software Badlands. While this is well applied in a 2D space, to enable more detailed practical research 3D processes need to be explored.

This is achieved in the open source Python package GemPy whose 'interpolation algorithm is comparable to implementations in commercial packages and capable of constructing complex full 3-D geological models' (de la Varga et al., 2019). GemPy uses a set of given points along the surface of each rock strata in the subsurface as well as that point's corresponding normal vector. These points, and the package's underlying methods, utilise cokriging for direct interpolation of the subsurface structure creating authentic lithological models. Modules such as GemPy, and similar packages Noddy and LoopStructural are useful but 'while these tools are invaluable in their respective scopes of use, they do not natively support large-scale randomization' (Ghyselincks et al., 2025). This is where another open source Python package StructuralGeo provides a solution. StructuralGeo uses Markov methods to generate a history of potential geological events, with each event being based on the previous, which yields a random geological history. This 'can generate a virtually infinite number of geological models with variable complexity and at any specified resolution, which can be used as data for a generative model' (Ghyselincks et al., 2025).

Despite all this progress, realistic geological modelling is still in itself a complex ill-posed problem (Garayt et al., 2025). One highlighted model, which utilised a General Adversarial Network approach, produces reasonably realistic 2D synthetic lithologies. These models prove easier to generate, however they lack the 3D realism essential to authentic geological applications as 'a difficulty for all the training image based techniques is to generate 3D fields when only 2D training data sets are available' (Coiffier et al., 2020). The 3D modelling program GemPy improves in the aspect of realism with its inclusion of fault simulation. However, there is an inherent reliance on existing realistic data points on the rock surfaces

as well as the inclusion of their normal vectors. This need for authentic information to develop a model extends the issues which come from a lack of quality labelled field data. While these points could be potentially randomly generated, this requires a depth of geological knowledge and further research to become applicable in the generation of synthetic datasets. Furthermore, although faults are included, representing their complex networks is still a challenge with a decent computational cost (de la Varga et al., 2019).

StructuralGeo presents a potential solution as it excels at generating structurally realistic geological models through its use of stochastic event simulation. (Ghyselincks et al., 2025). This package is limited though as it lacks a native inclusion of property assignment for different rock types. This means that features such as density aren't easily applied to the different layers within the model, limiting the direct applicability towards modelling gravitational data such as potential and acceleration. Additionally, being published in June of 2025, there is a limited amount of external research into the demonstration of StructuralGeo models realism in comparison to real-world data, although the paper specifies that it was tuned to be seen as "realistic" when visually determined by geologists.

There have been extensive advances in the development of synthetic geological models beginning from early surface observations expanded into the inclusion of detailed information from exploratory boreholes. During the maturation of the field a lack of detailed field data revealed itself as a key obstacle in the application of machine learning for geophysical applications. Synthetic datasets have been attempted to be applied with a Generative Adversarial Network approach leading to realistic, random 2D models but these lack dimensionality and elements of realism. GemPy provides a 3D alternative to model generation, with some authentic fault generation it is an improvement but it doesn't lend itself well to synthetic data generation due to its need for realistic data points to form the basis of the design. Finally, StructuralGeo provides improved random generation but doesn't inherently incorporate data such as density which is crucial to gravity modelling. Furthermore, being a newer package there is less research that has been done into its applications. Through this internship project I hope to develop a pipeline that can use the randomly generated models of StructuralGeo, with realistic applied properties, to train a machine learning network for the accurate modelling of gravity inversion.

# Data

There were three main sources for the data used in this research project. StructuralGeo was applied to generate all of the synthetic density data used in model training. PyTreeGrav performed the calculations to provide the surface gravitational acceleration measurements, together allowing for the primary training and validation of the neural network. With this synthetic data it was possible to get quantitative evaluation metrics against the ground-truth densities of realistic design. Contrastingly, the SEAM dataset functioned as an external test case to assess the fully trained models final performance on much more complex, industry-standard data, while still having a ground-truth density for final comparison of model performance.

## Synthetic Data

One of the key goals of this research project was the generation of more accurate synthetic geophysical data, so the vast majority of data utilised over the course of this project was generated using StructuralGeo. The key aspects of all datasets are discussed here, with the process of generation and randomisation further explored in the research section of this report.

There were five different geological designs implemented over the course of the research; insertions, basins, faults, salt bodies and mixed models containing a variety of the previous designs. Accompanying each of the geological density designs was the corresponding gravitational strength measurement at the surface of the model, which will be used as the input for the machine learning inversion. The five datasets, one for each feature type, all consisted of 3,000 different randomly generated (64, 64, 32) three dimensional models, as well as the 3,000 accompanying (64, 64), two dimensional gravitational surface data measurements.

The three dimensional data represents the densities of each voxel in the entire set and ranges from 1.80 to 2.87 g/cm<sup>3</sup> depending on the rock type (Alves et al., 2019).

The two dimensional data ranges from 249.78 to 388.41 mGal and represents the strength of the vertical gravitational acceleration for each pixel on the surface, based on all of the densities within the underlying model. All data was stored in the form of numpy arrays which were then reloaded and made into tensor format for application to machine learning.

## Insertions

One of the most common forms of insertion which is best represented here, is that of dikes. These are narrow, vertically orientated bodies of rock which cut discordantly through existing formations (Kavanagh, 2018). They typically have a differing density to that of the substrate around them. This density change combined with their distinct borders results in a recognisable gravitational anomaly at the surface which is ideal for attempting to predict with the neural network model.

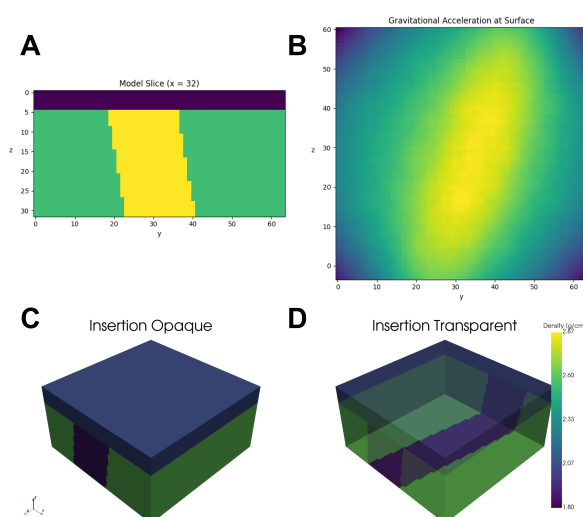


Figure 3. **A** is a 2D slice through the insertion model, **B** is the surface gravitational acceleration, **C** is the opaque plotting of the 3D density data, **D** is the partially transparent plotting of the 3D density data

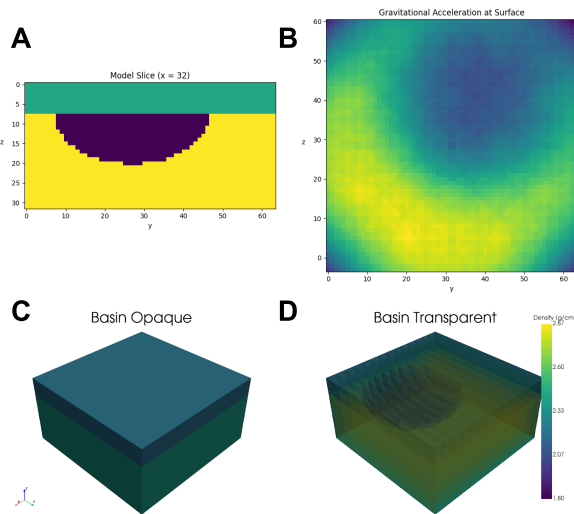


Figure 4. **A** is a 2D slice through the basin model, **B** is the surface gravitational acceleration, **C** is the opaque plotting of the 3D density data, **D** is the partially transparent plotting of the 3D density data

## Basins

Another common formation represented within the synthetic data is sedimentary basins. These are much broader low-lying areas comprising typically of lower density sediment to that of its surrounds (Rao, 1986). The flatter nature of these features produces much smoother, gradual change in gravitational measurement. The inclusion of these models allows for inversion to be tested against gradually varying density structures in contrast to the sharper more distinct features.

## Faults

Geological faults are shear fractures within a rock layer that can range in length over a broad range (Scholz, 2007). Similar to insertions these features present a distinct density change represented in a sharper gravitational distinction at the surface. One of the most common geological features due to constant movement of the Earth's crust, faults allow for a variety of angles to be explored including overhangs in connection with the dip angle of the fault.

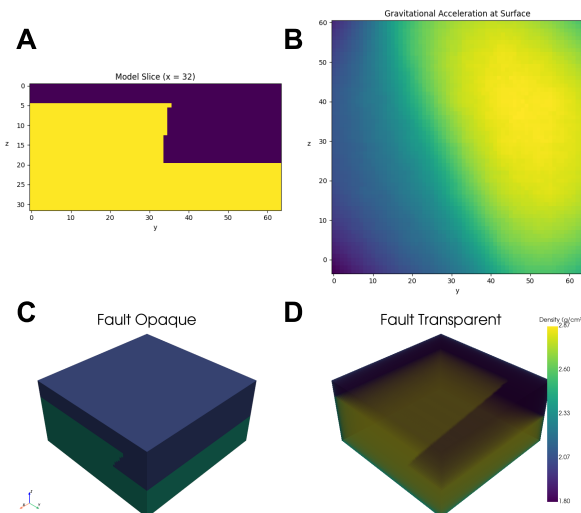
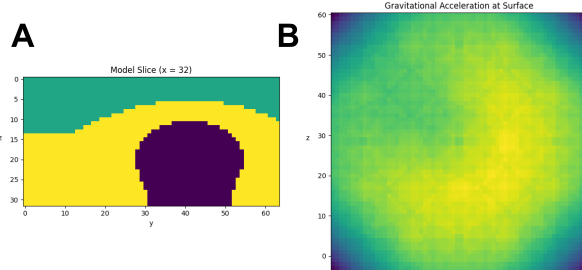


Figure 5. **A** is a 2D slice through the fault model, **B** is the surface gravitational acceleration, **C** is the opaque plotting of the 3D density data, **D** is the partially transparent plotting of the 3D density data



## Salt Bodies

An important formation in petrochemical exploration, salt bodies are large rounded features of a much lower density than the surrounding rock. Due to this lower density and overbearing pressure from other sediments the salt is displaced upwards (Hudec & Jackson, 2007). This results in unique formations ideal for identifying the

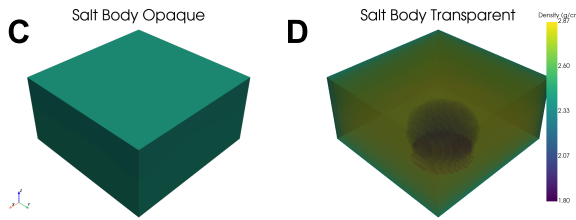


Figure 6. **A** is a 2D slice through the salt body model, **B** is the surface gravitational acceleration, **C** is the opaque plotting of the 3D density data, **D** is the partially transparent plotting of the 3D density data

model's capacity for more niche object identification, especially when in comparison to the rounded basins which produce a similar gravitational measurement in the form of the circular representation at the surface although the basins have slight signal difference which will hopefully be identifiable.

## Mixed Models

Finally, there is included a dataset of models containing mixtures of all the previous features. Representing increased geological realism as many of these features occur coincidentally with one another leading to density contrasts that happen at multiple scales and in differing regions of the model. The inclusion of interactions between features enables assessment of the model's ability to disentangle overlapping gravitational signals and presents a more authentic depiction of a neural network model's ability to function on real-world data.

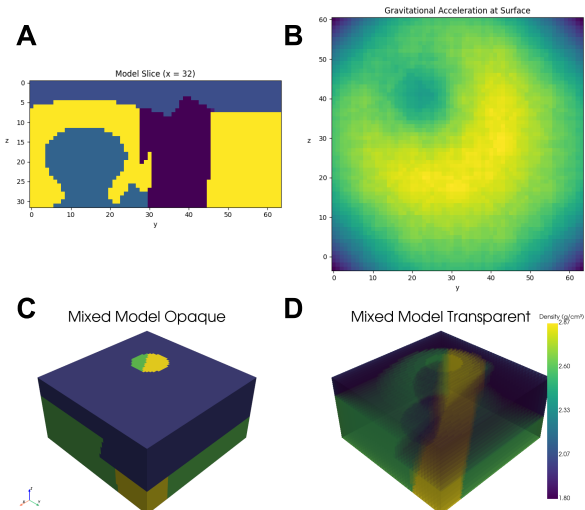


Figure 7. **A** is a 2D slice through the mixed model, **B** is the surface gravitational acceleration, **C** is the opaque plotting of the 3D density data, **D** is the partially transparent plotting of the 3D density data

## Real Data

For a final application of the neural network model a more complex, realistic dataset was acquired. This came in the form of the 2014 SEAM dataset. SEAM, SEG Advanced Modelling, was a consortium of petroleum companies with the primary objective to conduct geophysical modelling of relevance to the petroleum industry. They sought to design a “deepwater subsalt earth model designed to capture as much physics and realism as possible in a 3D model that was relevant to oil and gas exploration” (Fehler & Keliher, 2011). This resulted in a design, modelled inside Intrepid Geomodeller, representing a  $35 \times 40 \times 15$  km area of variable density simulations. The model consists of eight different rock types with different densities. These densities,

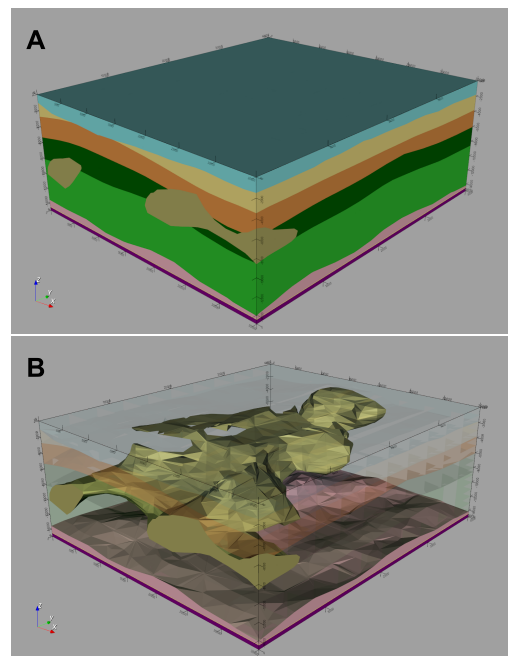


Figure 8. **A** shows the SEAM dataset in Intrepid Geomodeller, **B** shows the same dataset with only the salt body of interest visible.

which are input into Geomodeller with a standard deviation and mean value representative of true geological values tend to increase with depth and provide realistic values and formations for the layers surrounding a target feature. The main target of inversion, the salt body seen in Figure 8b, is much more complex than any training data previously described. It consists of a general upside down 'Y' structure, when viewed from vertically above but rapidly expands towards the centre depth. This expansion is continued by the branching off of segments of the lower density feature before the rapid contraction into a thin tower which connects to the base salt layer, visualised in Figure 8 as the pink lower layer. This is all representative of geological salt's natural incompressibility and tendency to deform under the high pressures of increased sedimentary layers (Hudec & Jackson, 2007) and so provides a keen insight into the applicability of neural network modelling to predicting real-world complex geologies.

While represented as a mesh model in Intrepid Geomodeller in Figure 8, when output as a voxel dataset the densities had a resolution of 56 x 60 x 30 with each voxel cube being a density value which ranged from 1.003 to 2.904 g/cm<sup>3</sup>. This constitutes each voxel representing approximately a 625 x 667 x 500m cube. The resolution of this data was chosen in consultation with a geoscientist at Intrepid, partly as it was the value used in the original conference from which the data was sourced and additionally as it allowed for the most effective constitution of the density data as this tended to be a pretty resource intensive process.

A noted challenge in this data was the fact that it was modelled at sea, resulting in a vastly lower density of the top layer which is representative of the salt water. This initially heavily impacted results as the model was trained all on on land data. However, this was adapted for by changing the density of this top layer, using Intrepid Geomodeller, to a value centred around 2.67 g/cm<sup>3</sup> with slight variations throughout the layer. This value was chosen as documents which accompanied the original dataset described this as the density required to create a gravitational output representative of the Bouguer gravity anomaly. This Bouguer anomaly is simply the gravitational acceleration measurements but if they have been corrected for topographical variations and other dependencies allowing for a measurement more reflective of the subsurface geological structures (Ayala et al., 2016). The final calculated gravitational data using this new density formation, exported from Intrepid Geomodeller, is seen in Figure 9 and has dimensions of 219 x 255 with values ranging from 1412.15 to 1447.20 mGal, noting a very subtle change of not even 40 mGal across this data. While not being a true reconstruction of real measured subsurface densities, this geomodel is created by experienced geophysicists from the SEG Advanced Modelling Corporation and provides a good baseline for neural network models performance on authentic data and its real-world applicability.

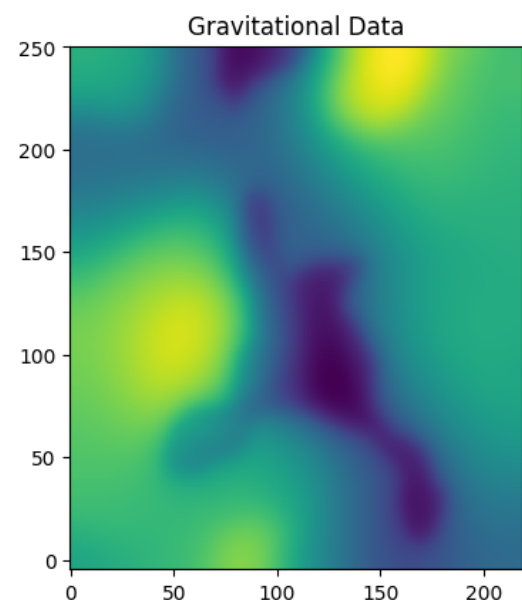


Figure 9. Gravitational acceleration at the surface of the adapted 2014 SEAM dataset.

# Research

The research within this project follows the pipeline depicted in Figure 10. Initially synthetic geomodels are created, which consist of a variety of geological features and which follow accurate geophysical constraints. This is continued by the calculation of the gravitational acceleration at the surface of each of these geomodels due to the densities of all rocks below. This combined dataset is then used to train a neural network to be able to predict any of the varying formations in the dataset. Ultimately, this model is tested on realistic data provided by Intrepid Geophysics. This structure allows the assessment of how machine learning performs on more realistic synthetic data and how this training process ultimately impacts the application to much more complex, final authentic data.

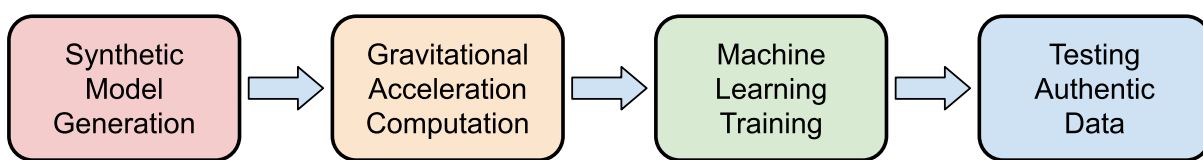


Figure 10. Pipeline for the research done over the internship.

## Synthetic Model Generation

In order to generate sufficient synthetic data for model training, StructuralGeo was utilised due to its beneficial use of geological histories when creating synthetic models. These histories mean that geological features can be added to the model in any desired order and have realistic effects on all of the properties which have already been applied. StructuralGeo also easily lends itself to variable resolution and complexity in the designs which allows for experimentation to find the optimal size and intricacy for efficient data generation and modelling. Additionally, the voxel grid which StructuralGeo natively exports, can act as the input to gravitational acceleration calculation program PyTreeGrav. This all allows for improved flexibility within the model designs as well as increased realism which will ideally improve the final neural network performance.

## Insertions

To capture the disruptive nature of an igneous intrusion within sedimentary sequences a dike feature was inserted into some synthetic models. Chosen due to their nature as key components of intrusion networks, these features “have implications for understanding aspects of geology as diverse as volcanic hazards and the formation of some of the world’s most valuable ore deposits (Dering, 2020).

This feature originates within the lower sedimentary, or basement layer, and extends upwards through the formation before being covered with a final sedimentary top layer. It is also assigned a density higher or lower than its surrounding rock type to represent different types of intrusion, as visualised in Figure 3. Lower sedimentary layers were assigned values ranging from 0 to 3, insertion values were either 10 or 11 and top sedimentary layer ranged from 4 to 8. The variation in insertion depends on strike and the dip symbolising the angle at which the insertion is rotated and the amount of slope it has respectively.

## **Basins**

These features, similar to the insertions, originate in the lower sedimentary layer but only reside near its surface in the hemispherical shape depicted in Figure 4. They are chosen as an avenue of synthetic data exploration as they “play a crucial role in the generation, migration, and accumulation of hydrocarbons, forming the foundation of global petroleum systems” (Alamu & Dada, 2025).

The basin is also assigned a density higher or lower than its surroundings, representative of the contrast in rock types. This is then covered in another final sedimentary layer of top soil deposition. Again, lower sedimentary layers received values from 0 to 3, the basin itself was either 10 or 11 and the surface sedimentary layer ranged from 4 to 8. In this formation key variations stem from the randomly generated height of the basin as well as its semi-major axis which alters how elliptical the depiction is.

## **Faults**

These features differ as they are not the addition of another material in the base sedimentary layer, but rather a deformation of it. Faults are one of the most commonly occurring geological structures, formed by the movement of tectonic plates they generate on a variety of scales but remain points of significant subsurface change and movements which may result in both seismic and aseismic behaviour (Micklethwaite et al., 2010).

A higher density lower layer is deformed by a fault leaving a ‘step’ in the formation. This is then covered in a top sedimentary layer filling the rest of the model. The sedimentary values vary from 0 to 3 and 4 to 8 once again with the unique features of the fault stemming from the randomly assigned strike and dip angles, seen in Figure 5, similar to the method applied for insertions.

## **Salt Bodies**

More uniquely shaped than other geological features, while salt bodies are traditionally a target for highly productive fossil fuel resources they also “provide excellent opportunities for developing economically viable clean energy systems” (Kernen et al., 2024). Salt bodies are formed when the pressure exerted on lower density salt by upper sedimentary layers becomes too great, forcing the layer to find its way through cracks in upper layers. This viscous nature of salt means it is able to trap hydrocarbons under the large domes and overhangs it forms underneath the ground (Grunnaleite & Mosbron, 2019).

One of the more complex features to design in StructuralGeo, salt bodies first require the parabolic folding of the base sedimentary layer, to be representative of the thrusting effect rising salt has on covering layers. The uniquely shaped salt dome itself extends upwards from the bedrock through the base sedimentary layer almost reaching its surface. The salt domes are assigned a lower density than all the surrounding rocks to realistically represent the more fluid nature of the material. This is again covered in a final sedimentary surface layer. The base sediment is now assigned a value ranging from 0 to 2 with the surface sediment ranging from 3 to 5. The salt dome itself is always assigned a value of 6 which later becomes representative of the lower density of the material.

## Mixed Models

Finally, the most intricate features for model training and prediction were a combination of all or some of the previous features. Designed to be representative of the complex geological effects that multiple features can exert on one another within the same area, these designs present a more authentic exploration of how the previous feature may appear out 'in the field.'

There are 16 different possible historical feature lists to choose from. Each list is simply a realistic geological ordering of potential features, for example `["basin", "salt", "insertion", "fault"]`. These lists were then chosen at random and the features were added with their previously defined characteristics maintaining a respect of geological ordering with younger features cutting through older ones to remain representative of realistic effects.

## Post-Processing

Before any gravitational acceleration calculations could be performed, the assigned formation values which currently represented each rock type as a single integer ranging from 0 to 11, needed to be replaced with realistic densities so that the forward modelling equations would result in realistic values. These densities were assigned according to [Table X](#), with the chosen densities being taken based on a 2019 report by Alves et al. and increasing with their relative depth within the geomodel. Of course in reality the density of rock lithologies varies significantly depending on the pressure applied from above and the conditions in which they are formed, these distinct values were chosen for simplicity of testing the initial model while still maintaining general geological realism.

Integer Value	Assigned Density (g/cm <sup>3</sup> )	Potential Rock Counterpart
0	2.62	Quartz
1	2.54	Gypsum
2	2.42	Chalk
3	2.39	Limestone
4	2.34	Sandstone
5	2.19	Soil
6	2.05	Salt
7	2.01	Shale
8	1.80	Silt
9	2.45	Dolomite
10	2.87	Hornblende
11	1.89	Clay

Table 1. Densities corresponding to each integer value and their real-life rock counterpart, adapted from Alves et al., 2019

## Gravitational Acceleration

After many attempts with alternative open-sourced programs, PyTreeGrav was ultimately used for the calculation of gravitational acceleration at the surface of each model. This is due to its variable calculation methods as well as targeted calculation areas so it doesn't need to calculate for the entire model, only the area of interest. PyTreeGrav is also able to automatically select the fastest method for gravity calculation with an "exact direct-summation ("brute force") solver and a fast, approximate tree-based method that can be orders of magnitude faster" (Grudić & Gurvich, 2021). This is vital as each pixel on the surface, which is being calculated for, needs to factor in the effects which every density value cube in the entire model has upon it. Additionally, it proved much easier to install and implement than other methods further improving efficiency throughout the research. Results of these gravitational acceleration calculations can be seen in Figures 3 through 7 in the Data section.

## Edge Effects

Each model, while being finalised to be (64, 64, 32) in the (x, y, z) dimensions, begins as a (96, 96, 32) sized geomodel in order to address the edge effects which commonly come into factor when calculating gravitational data on a small region of density data. This is due to the fact that PyTreeGrav treats the model as being surrounded in empty space, meaning that towards the edges of the defined models there is less mass causing a gravitational effect, resulting in a tapering strength of measurements as seen in Figure 11. By simply extending the domain of the model beyond the target area we obtain more realistic results for inversion training, similar to methods used within other papers exploring gravitational calculations (Witter et al., 2016).

The dimensions of (96, 96, 32) were chosen through trial and error as they were found to allow for the most details in the final outcome while still maintaining minimal computation time. It was also ensured that no key features would be fully cut off from the final density model by roughly centering them, despite their randomised position in the initial model. Some features appear along the borders of the newly defined area but they still present their gravitational effects in the final calculations.

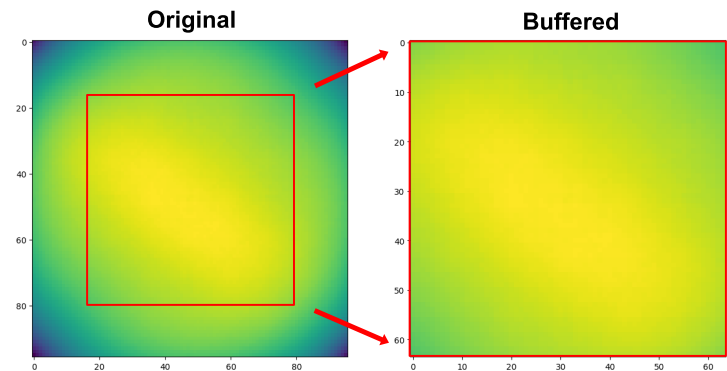


Figure 11. Original gravitational data with visible edge effects compared to the buffered data.

## Machine Learning

In order to obtain accurate geological modelling from the surface gravitational data, an appropriate neural network architecture had to be chosen and designed which can capture the complex nuances of inversion. For this, a Convolutional Neural Network design was selected. This was chosen through a variety of research as it was found that the vast majority of recent effective papers implemented this design or something similar (Li et al., 2023; Wu et al., 2023; Zhou et al., 2024). Potential alternative model designs were

hypothesised and partially tested, but it was hoped that the implementation of this, proven to be effective methodology, could be improved upon and provide unexplored research benefits.

## Architecture

The design for this model was inspired by the methodology implemented in a 2024 paper from Zhou et al. which showed success in applying machine learning to gravity inversion but only utilised simple geological models. The architecture, pictured in Figure 12, consists of an encoder on the left which extracts features of the gravitational acceleration input, and a decoder on the right, which upsamples those key features in the final density predictions.

The encoder aspect of the network is a series of downsampling processes which consists of four identical operation sections. In each, a two dimensional convolution is applied over the input which keeps the x and y dimensions the same but expands the channels to obtain a representation of the density underneath the surface. This is followed by a batch normalisation layer and a ReLU function which helps to stabilise the model training. This process happens twice in each of the four submodules with the convolutions utilising a kernel size of (3, 3), a stride of (1, 1) and padding set to “same” in order to capture the most detailed relationships in the data. A max pooling layer then does the actual downsampling of the data, reducing computational cost but maintaining the key features obtained by the convolutions. This is continued until reaching the deepest layer of the network, ideally this now contains a representation of all of the most important surface features and their corresponding density density responses.

The encoder is followed by the decoding process. The decoder is symmetrical to the encoder but employs an upsampling design to take in the now (4, 4, 1024) data (x, y, channels) and increase it back up to the original dimensions of (64, 64, 32) with the new 32 channels representing the desired density information, thus becoming (x, y, z). Additionally, skip connections included in this upsampling process ensure that information is preserved from the original input and is actually being effectively added into the output. Ultimately, this whole process results in a change from the (64, 64, 1) input to the final (64, 64, 32) output.

## Curriculum Training

In order to learn the simple features of the key datasets and to be able to identify them within a more complex geological environment, a curriculum training approach was implemented for the model training.

This strategy, mimicking human learning, trains the machine learning model from easier to more difficult data and has “demonstrated its power in improving the generalization capacity and convergence rate of various models in a wide range of scenarios” (Wang et al., 2021).

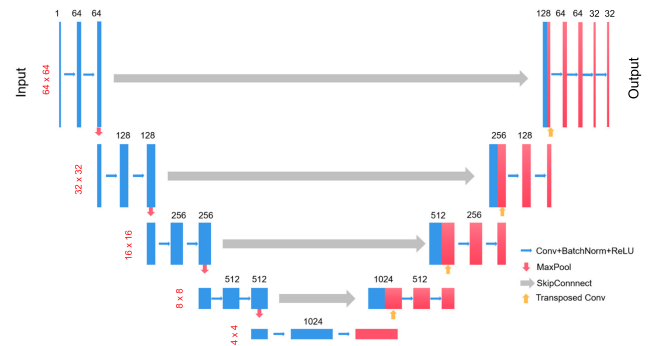


Figure 12. Architecture of the implemented convolutional neural network used for prediction, adapted from Zhou et al., 2024.

The original sets of data featuring 3,000 models for each different geological design were repurposed to form the inputs for each different stage of the training based on how complex they were, and how difficult initial experimentation showed they were for the model to learn.

- Stage 1
  - Insertions
  - 3,000 density and gravity models
- Stage 2
  - Insertions + Basins
  - 6,000 density and gravity models
- Stage 3
  - Insertions + Basins + Salt Bodies
  - 9,000 density and gravity models
- Stage 4
  - Insertions + Basins + Salt Bodies + Faults
  - 12,000 density and gravity models
- Stage 5
  - Insertions + Basins + Salt Bodies + Faults + Mixed Models
  - 15,000 density and gravity models

Every stage of the curriculum is simply adding data to train the model on, which essentially fine-tunes the parameters based on the previous stage, but still employs the same model. Each stage was split into 80-10-10% training, validation and testing subsets, using a batch size of 64 for optimal convergence of model parameters as well as Adam optimiser for the model learning. Before being used in this training process all data was also normalised for a more equal contribution of features as well as faster convergence of the algorithm. Early stopping was implemented when plateauing was seen within the model losses per epoch, through analysis of the training and validation loss. Ultimately, this seeks to result in one versatile model which is able to accurately predict any of the different geological feature types.

## Realistic Data Testing

For the final stage of the research process the model, now fully trained on synthetic geological data, was applied to the vastly more realistic 2014 SEAM dataset in order to measure potential real-world applicability. Due to the neural network taking in a 64 x 64 input and the gravitational data being 219 x 255 two different potential approaches were applied.

### Patches

First, a patch-based approach was applied to predicting from the new data. This involved passing each possible 64 x 64 patch of the entire 219 x 255 input into the neural network model to get its predictions for the entire gravitational data. Where these patches overlapped the average was taken to get the combined final prediction for the entire geomodel. This method, while intuitive in the sense of application, loses some physical realism. This is because the synthetic data, while generally scaleless in the model training phase, was modelled on a much larger scale than what a 64 x 64 section of the gravitational input represents. This results in the predicted density output being less directly comparable to the

true densities. Additionally, this approach may struggle with the global features of the true model as each prediction is being conducted on a much smaller prediction area. Contrastingly, this method may have better performance in the capture of intricate details within the geomodel design and is still applied in this report to get a sense of how this approach captures shapes where bodies of interest may lie and for exploration of all possible methods.

### Downsampling

Alternatively to the patch-based approach, downsampling was used to adapt the uniquely shaped data to be input into the neural network model. This involved simply rescaling the input from  $219 \times 255$  directly to  $64 \times 64$ . This loses resolution of the input but means that better geospatial relationships are retained when predicting, it will ideally be able to better understand the broader shape of key structures. Additionally, this means that the input is much closer to the scale of the training data, allowing for the preservation of physical realism. This means that results can be almost directly compared to the true densities.

Finally, for better interpretation the output was resized to match the size of the true densities array. This doesn't lose the accuracy of any geological predictions, but simply changes the scale of each cell in the predictions. This is acceptable as we are more interested in how well the model can capture general subsurface geological shapes as opposed to exact densities.

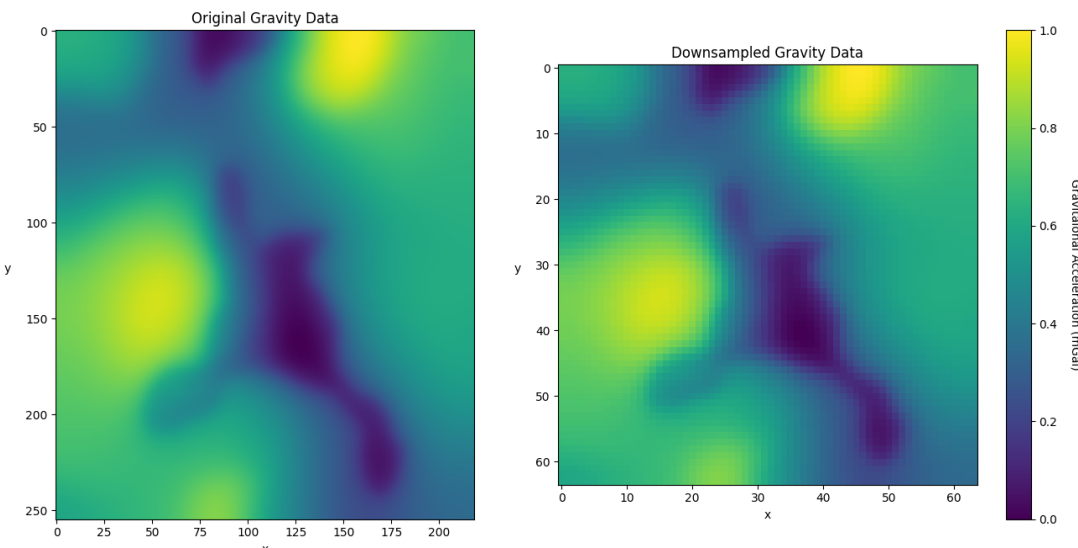


Figure 13. Original gravity data on the left compared to the downsampled, lower resolution gravity data. Both have been normalised resulting in a scale of 0 to 1.

# Results

## Curriculum Training

Throughout the process of curriculum training the time per epoch increased drastically with the additional data in each stage, this was to be expected due to the increasing information the model has to iterate through however still made the training process more difficult. Each stage of model training presented similar trends in the improvement of training and validation loss with values dropping rapidly then presenting slower improvement over the next few epoch before plateauing later on as seen in Figure 14. The validation losses presented much more oscillation, presumably due to the smaller sample size but still tended to trend downwards. Additionally, early stopping was implemented when each training stage appeared to be stagnating in its improvement of the validation loss values. This helped to save time and resources in the training process, but also prevents overfitting to the training data. Examination of the validation loss throughout the training process allowed for the prevention of overfitting as it stayed consistent in its descent with the training loss. The addition of a dropout layer as a further prevention for overfitting proved unnecessary with analysis of these results. Exact values for the final test loss and  $R^2$  scores are seen in Table 2.

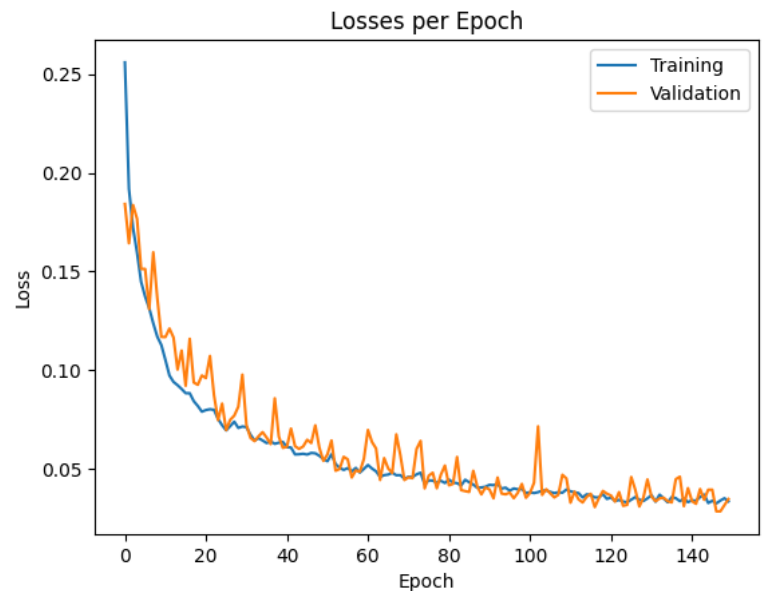


Figure 14. Training and Validation losses for Stage 1 of the curriculum training process.

Stage	Training Time	Number of Epochs	Test Loss	Test $R^2$
1	33m 5.7s	150	0.0349	0.9141
2	27m 44.1s	62	0.0307	0.9102
3	39m 30.3s	55	0.0215	0.9186
4	56m 10.6s	51	0.0240	0.9109
5	80m 29.7s	72	0.0230	0.9067

Table 2. Training times, epoch counts, test loss and test  $R^2$  score for each stage of the training process.

Overall, the model exhibited stable convergence throughout the curriculum, with the test loss decreasing overall and the  $R^2$  values remaining consistently over 0.90. Stages 3 to 5, which started to involve more complex geological structures, required longer training times to reach an optimal plateau of validation loss. The number of epochs also decreased throughout as the model was building upon the work done in all of the previous stages, so each new addition was more of a fine-tuning process and each epoch became longer to process through. This is contrasted in the final Stage 5 training however as it was sought to give the model further training time to ensure it really achieved an optimal amount of accuracy in its density predictions.

Despite the added complexity, the model managed to maintain a high predictive accuracy indicating a successful transfer of knowledge from the simple to more complex datasets. A final testing loss of 0.0230 with an  $R^2$  score of 0.9067 was achieved which shows that the model is able to capture the vast majority of the variance in the true density values, combined with the low L1 test loss this presents potentially good generalisability to new, more complex datasets.

For additional comparison, the same model architecture was trained on just the dataset of the 3,000 most complex mixed models which resulted in a test loss of 0.0836 and an  $R^2$  score of 0.6766. The same model architecture was again trained, but this time on the full stage 5 dataset containing 15,000 different models. However this time it was without having been through the first 4 stages of curriculum training and this resulted in a test loss of 0.0333 and an  $R^2$  score of 0.8582. While not presenting a vast difference in results to the full implemented approach the 5% increase in accuracy could provide distinct benefits in real world field applications, saving time and resources, and justifies the use of curriculum training. While the achieved final quantitative results are consistently well performing, when applied in geological contexts a visual inspection is just as important, if not more important as this is how it is applied in the geophysics industry. It is crucial to ensure that general geological shapes are being captured for the true context of where different features lie.

## Synthetic Data Insertions

In Figure 15 it is seen the model's successful ability to capture the position of insertions. This was expected due to the distinct nature of the associated gravitational acceleration measurements which are input into the model. However, the model also shows success in capturing the dip angles of various insertions at various depths which is a much more difficult task given the very slight effect the changes in angle give to the gravitational input.

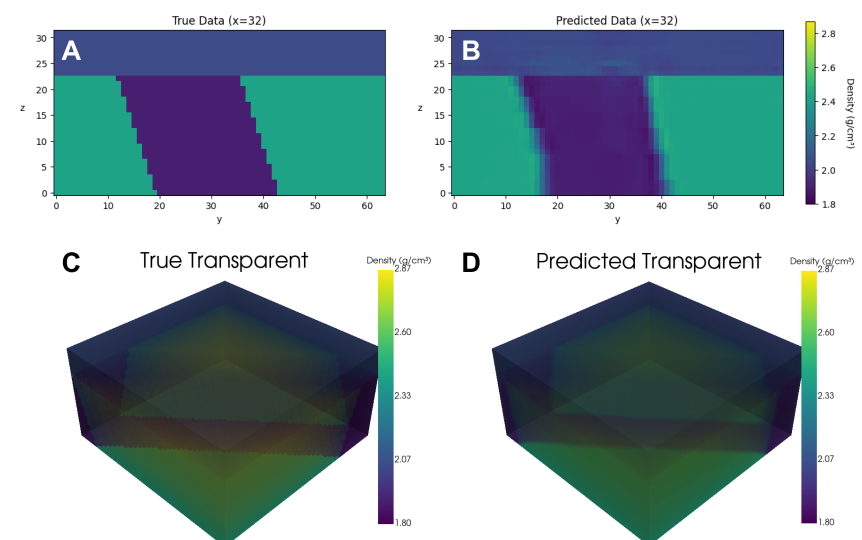


Figure 15. **A** is a 2D slice through the true density data, **B** is a 2D slice through the predicted density data, **C** shows the full 3D true model data, **D** shows the full 3D predicted model data.

## Basins

These rounded features present a slightly more difficult, subtle design for the model to predict as seen in Figure 16. The neural network is able to relatively accurately determine the depth of these basins but struggles somewhat with the rounding of the structure.

Though it struggles with the details, the model is still successful in its predictions of the basin position and general dimensions in the subsurface.

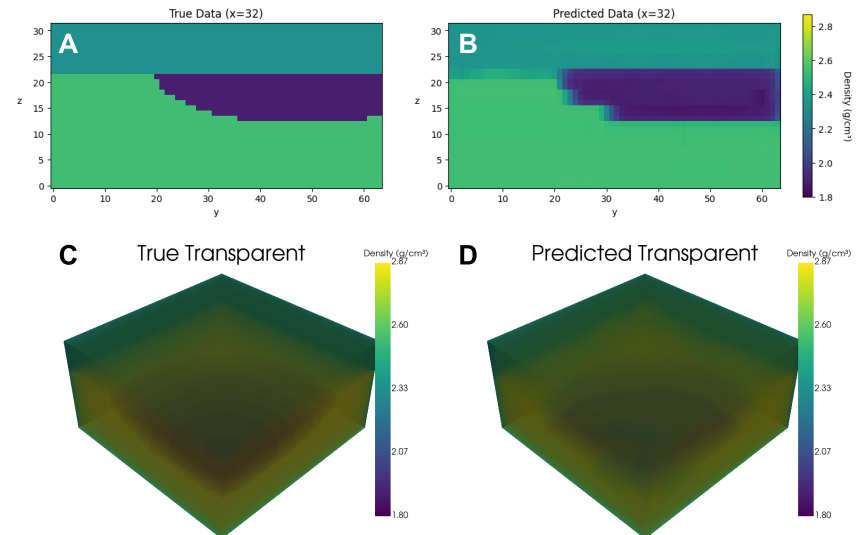


Figure 16. **A** is a 2D slice through the true density data, **B** is a 2D slice through the predicted density data, **C** shows the full 3D true model data, **D** shows the full 3D predicted model data.

## Salt Bodies

Similar to the prediction of the previous basins, the neural network model is able to accurately identify the positions of these salt bodies in a variation of randomised forms.

However, it is seen to struggle with the precise definition of the borders of the feature, not quite capturing the curve of the lower sedimentary layer and the rounding of the salt body feature as seen in Figure 17. Difficulties are further seen in the concavity in the bottom half of the feature where the model increases in lost realism. This is disappointing as this is a key location for the storage of natural oil and gas but the general position and dimensions of salt body predictions were seen to be correct.

Additionally, the model succeeds in identifying the difference between these salt bodies and the previous basins, despite their similarity in at surface gravitational accelerations.

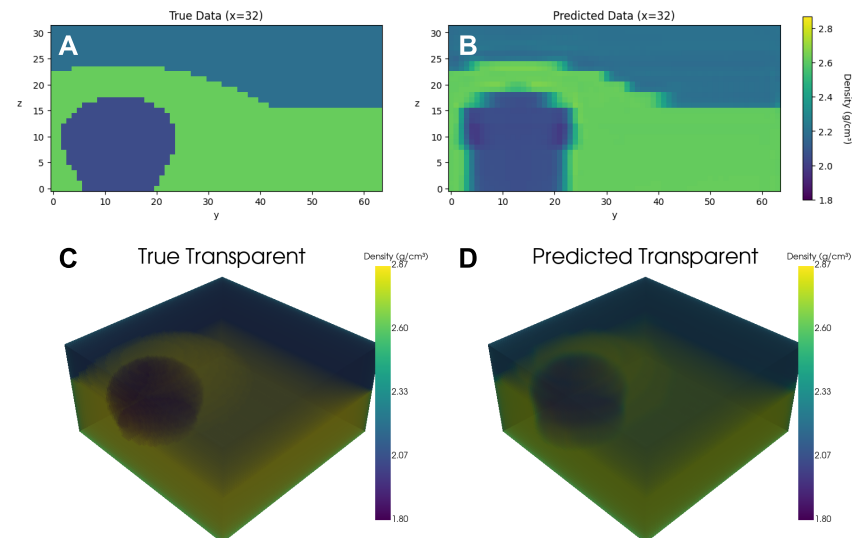


Figure 17. **A** is a 2D slice through the true density data, **B** is a 2D slice through the predicted density data, **C** shows the full 3D true model data, **D** shows the full 3D predicted model data.

## Faults

Presenting another more distinctly vertical feature, similar to insertions, the model proved successful in its ability to locate faults and follow their geology closest to the surface. It can be seen in Figure 18 that difficulties arise in the capturing of the true angle at which the fault dips. This is likely due to the similarity in gravitational reading of a positive slope angle to a negative one, however the model was able to correctly predict this angle for earlier insertion models so this is disappointing. The model performs reasonably well at identifying the depth of the lower part of the faulted feature when taking into consideration the minimal effect on surface gravitational measurement which is occurring from a density change at this depth.

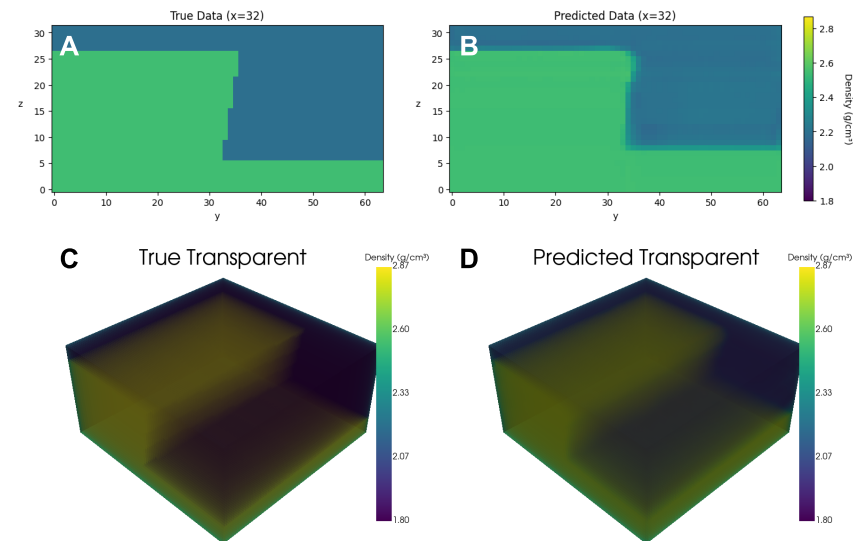


Figure 18. **A** is a 2D slice through the true density data, **B** is a 2D slice through the predicted density data, **C** shows the full 3D true model data, **D** shows the full 3D predicted model data.

## Mixed Models

Finally, the fully trained model shows relative success in its predictions of the more complex mixed model designs. Contrasted to the previous design predictions it is visible in Figure 19 that the boundaries between objects now have become much less defined. This is due to the increased interference which all the additional features are having on the final gravitational acceleration signal. However, while it struggles to perfectly forecast the exact dimensions, the general locations of key features are being well identified which shows promise for the real world applicability of the model, especially with the detection of the slight variation in density visible above the position of the salt body in Figure 19.

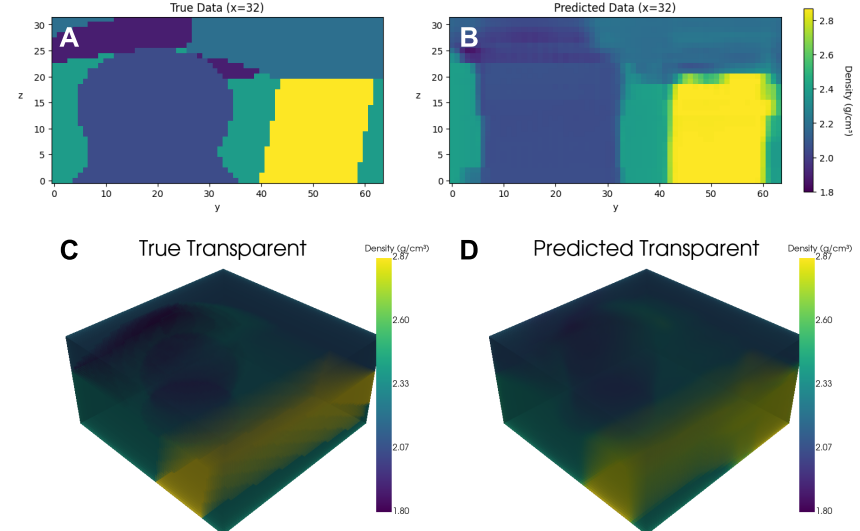


Figure 19. **A** is a 2D slice through the true density data, **B** is a 2D slice through the predicted density data, **C** shows the full 3D true model data, **D** shows the full 3D predicted model data.

## Realistic Data

Utilising the 2014 SEAM dataset described in the data section, the two approaches of predicting by patches and through downsampling the gravitational acceleration data were both explored.

### Patch Predictions

When viewing the side-on slice taken comparing the predicted against the true densities in Figure 20, it can be seen that the model clearly struggles significantly with this approach. The densities approaching the surface are especially dissimilar, which is similarly reflected across most of the vertical slices taken from the predictions. However, visible round  $x = 85$  it can be seen that there is a change in density across the predicted and the true data presented what may be some successful anomaly detection, but it remains difficult to tell. Another beneficial way to examine this data is viewing top down, to see if the general shape of that salt body of interest is being captured.

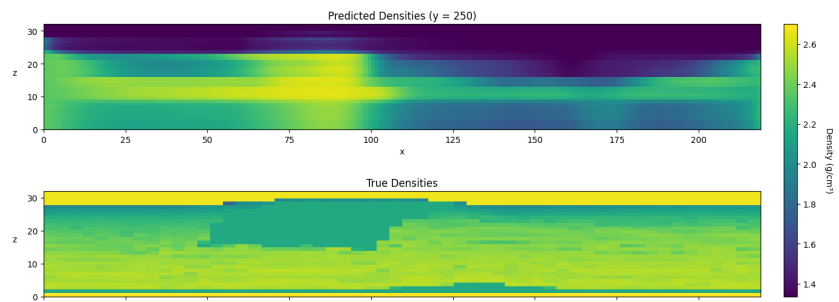


Figure 20. Predicted densities (top) compared to true densities (bottom).

As the predictions first begin to go under the surface in Figure 21a, this is where it would be expected that there is the most geological accuracy as the features closest to the surface have a larger impact upon the surface gravitational acceleration measurements. It is seen however, that the predictions are very different in their densities compared to the true, much higher value. The edges of the distinct salt structure are slightly discerned but not nearly as much as the true values.

This is similarly reflected in Figure 21b, with slightly more of the shape of interest being identified, however the differences in density continue.

A third of the way deep into the predictions in Figure 21c, it is seen that the model is indeed successfully capturing some of the distinct upside down 'Y' structure of the salt body with a promising increase in density as the depth increases.

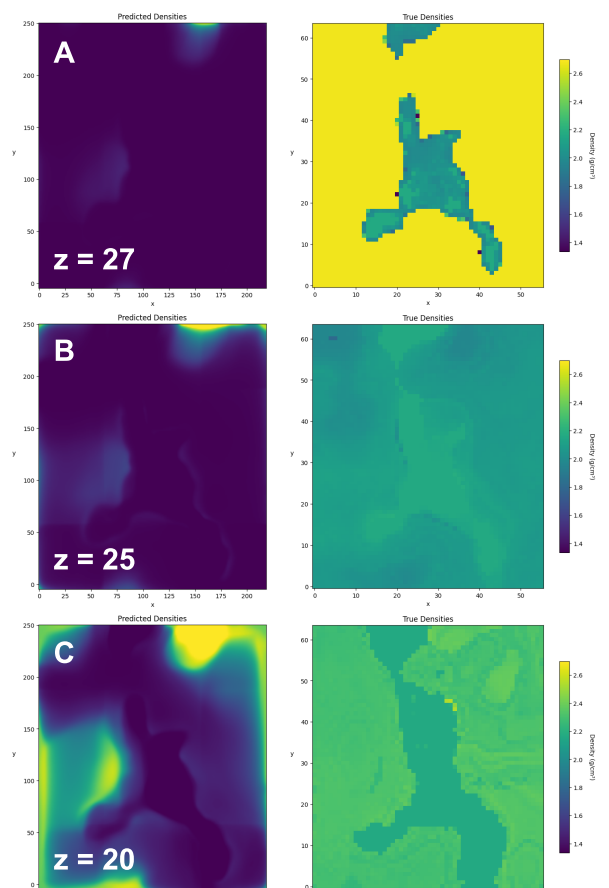


Figure 21. Predicted, compared to true density values at increasing depths. Each z level is roughly 500m.

Predicting now halfway through the depth of the model, at a corresponding depth of around 7.5km, it is seen that the predictions continue their slight increases in density value with the further propagation of that predicted shape in the centre. But the true values show that target structure has begun to widen out and this change is not reflected in the prediction as seen in Figure 22a.

Now at a depth two-thirds of the way into the structure, in Figure 22b, there is a jump in average density predictions which correlates with the true density values but the body of interest has really lost any semblance of representing the authentic shape.

Finally, at a depth just above the lowest level, in Figure 22c the predictions are almost entirely different from their expected values. While this is understandable due to the increasingly weakened impact structural changes at this depth have on at surface gravitational readings, it was hoped that the average density would be more representative of the true data as seen in the synthetic models.

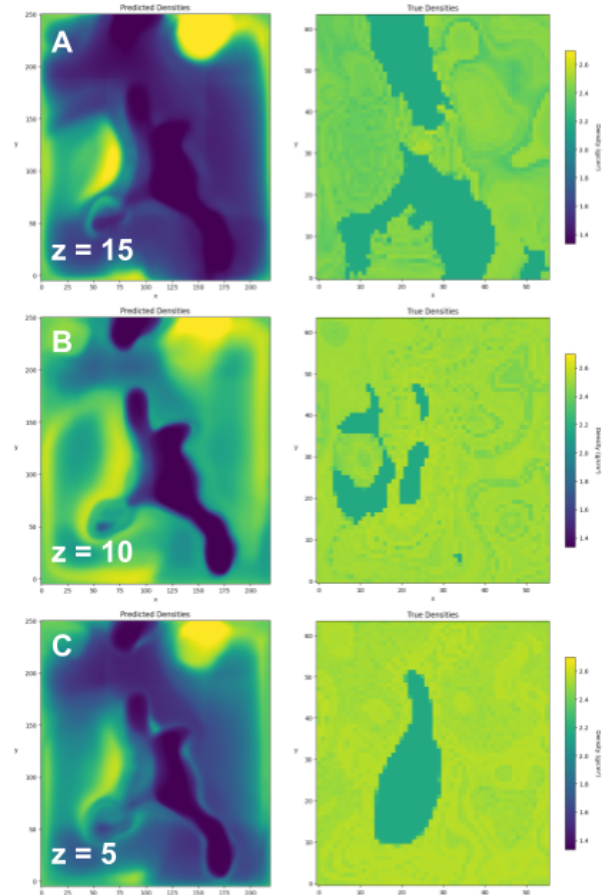


Figure 22. Predicted, compared to true density values at increasing depths. Each z level is roughly 500m.

## Downsampled Predictions

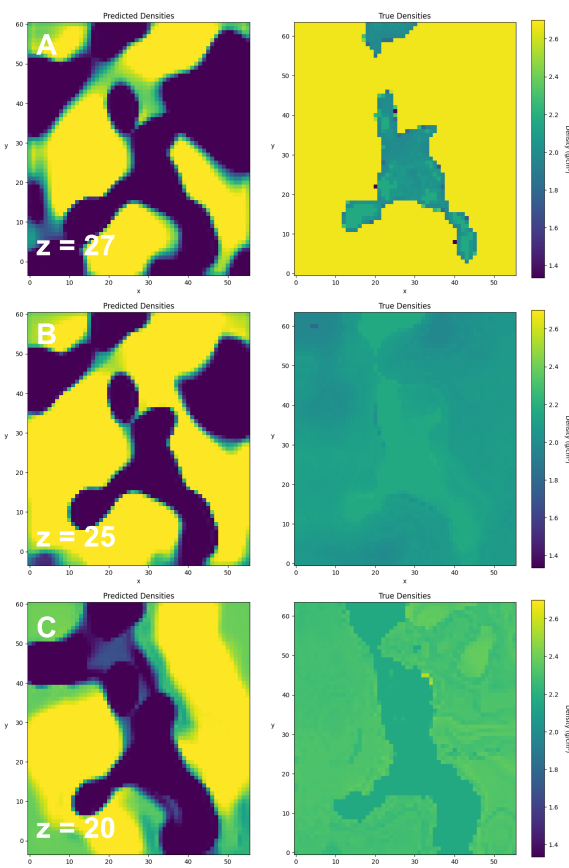


Figure 23. Predicted, compared to true density values at increasing depths. Each z level is roughly 500m.

Following the same increases in depth as with the previous patch sampling approach, just below the surface, as seen in Figure 23a, it is clear that this prediction method is already producing an improved reconstruction of the true structure. While there are still some strange low density areas in contrast to the constant surrounding high density of the true information, the shape of the salt body structure is being captured much earlier than in the previous attempt. Further down into the predictions, in Figure 23b we see the background densities begin to stabilise but they still remain unrepresentative of the true densities in the feature. Now a third of the way into the full depth of the model, Figure 23c presents an interesting depiction in the changing and expanding form of the predicted structure. Where the previously implemented patch-based approach just continued the initial shape down throughout the whole model, this downsampling method results

in the predicted shape changing with the increased depth and appearing much more representative of the true values.

In Figure 24a it can be seen that the predicted structure of the lower density body of interest is continuing to expand which is somewhat reflected in the true data, especially in the similarities in the lower right area of the figure.

Now two thirds into the depth of the model with Figure 24b, it is clear that the prediction is losing realism as where the true salt body experiences a quite sudden, drastic narrowing that isn't seen in the neural networks predictions. There is a slight increase in the density of certain areas on the predicted body of interest but not a true restructuring that would ideally be represented. Finally, at the near lowest level it is clear that the prediction has suffered similarly to the patch-based approach, with the decreased impact on the surface gravitational acceleration that any changes in true structure or density would have at this depth. This can be seen in Figure 24c.

Overall, through an extensive visual comparison of the outputs from the patch based approach and the downsampling method, it is evident that the downsampling method had more success in capturing the true structure of the body of interest.

This is especially keen in the depiction of the changes in structure that come with increasing depth, showing much improvement in capturing these. However, going below half depth ( $z = 15$ ) both approaches struggle significantly with the sudden changes in formation and are unable to accurately capture the design. Both approaches seemed also to struggle with getting accurate predictions for the density of the subsurface. This may be due to the complexities of this professionally designed dataset, however particularly the downsampling method appears to suffer from scaling difficulties, with the high densities being too high and the low densities being too low. Ideally with further fine-tuning and more realistic data this could be tuned out and an accurate relationship between these inputs and outputs will be learned.

Although both approaches suffered difficulties, the successful general mapping of the anomalous lower density structure proves promising for further research and potential authentic applications.

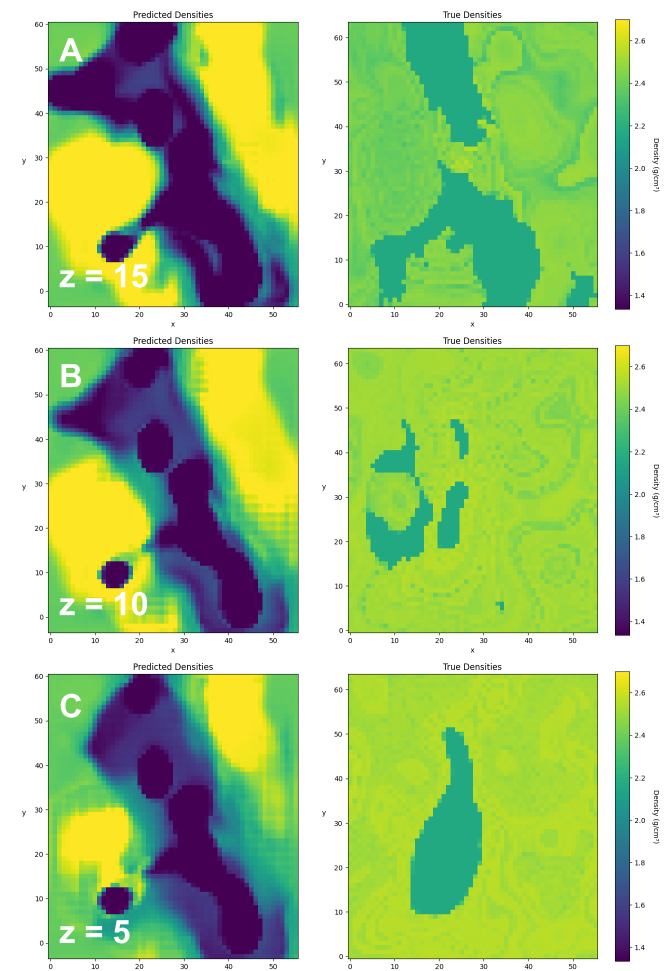


Figure 24. Predicted, compared to true density values at increasing depths. Each  $z$  level is roughly 500m.

## Conclusion

This report aimed to develop an efficient pipeline for the synthetic generation of geological models that more accurately mimic real-world complexity through the incorporation of realistic geological and geophysical prior information, as well as data-driven realism constraints. The gravity responses corresponding to these models were then to be used to test the effectiveness of these synthetic datasets for training a geological machine learning model in predicting three dimensional subsurface density from two dimensional surface gravitational acceleration data. Finally, the model was evaluated using realistic geological data.

The generation of synthetic geomodels was streamlined using StructuralGeo and its naturally incorporated realistic geophysical information. This allowed the development of an efficient pipeline for the generation of five synthetic datasets including faults, insertions, basins, salt bodies and a mixture of these features. Accompanying each of the synthetic density models was the calculated gravitational acceleration at the surface, using PyTreeGrav and buffering to reduce edge effects. The proposed CNN U-Net architecture, in conjunction with a curriculum training approach, achieved consistently stable inversion performance when tested on the synthetic datasets. When tested on the authentic 2014 SEAM dataset the predictive model showed success in capturing the general shape of the body of interest but struggled in achieving truly representative densities.

These results show the applicability of more realistically designed synthetic datasets to geophysical inversion, especially to help address the scarcity of true geological data. The successful performance on all synthetic data as well as the potential seen in the more realistic final test provide a viable path towards truly accurate inversion and, in turn, more efficient resource exploration.

While promising and able to generate more realistic geological structures than previous research into the field, this approach still struggles with the true complexity of real-world structures. The variety of initial conditions and features that can occur remain a challenge to capture in any sort of training data. Additionally, it was seen that there were significant deviations in the predicted density values when compared to the true subsurface densities of the SEAM dataset.

Moving forward, further research into this project would hope to utilise more datasets similar to the realistic SEAM model to try and fine tune the neural network parameters. This could help to address the scaling issue with the density predictions, as well as introduce some of the finer details of these more complex designs. The addition of more computational power would allow for the potential inclusion of additional geophysical data such as magnetic measurements. Also, further collaboration with geophysicists could increase the realism of the synthetic training data and allow for the introduction of a true physical scale which would help to know the area of applicability for this predictive model, while also making it easier for anyone using the predictions to understand the area they are working with.

Overall, the research done over the course of this internship has demonstrated the feasibility of using more realistic synthetic data for training a machine learning model to perform

geophysical inversion. It has also been seen how this synthetic data improves the geological realism of the predictions compared to previous research which locates general anomalies. The project provided some valuable insights into the challenges of generating such extensive, geologically accurate, synthetic data for neural network training. Finally, application to the 2014 SEAM dataset shows that when implemented correctly, the inversion network can successfully delineate the position and changing shape of a lower density body interest, presenting a pathway for further use of machine learning for effective resource exploration.

## References

- Alamu, R., & Dada, O. J. (2025). *Sedimentary Basins and Hydrocarbon Accumulation*.
- Alkhalifah, T., Wang, H., & Ovcharenko, O. (2022). MLReal: Bridging the gap between training on synthetic data and real data applications in machine learning. *Artificial Intelligence in Geosciences*, 3. <https://doi.org/10.1016/j.aiig.2022.09.002>
- Alves, E., Fernandez, T., & Cersosimo, S. (2019). *FEASIBILITY STUDIES AND ELASTIC INVERSION APPLIED TO GEOPHYSICAL CHARACTERIZATION OF THE OFFSHORE TARANAKI BASIN, NEW ZEALAND*. <https://doi.org/10.13140/RG.2.2.31464.49924>
- Ayala, C., Bohoyo, F., Maestro, A., Maria Carmen Reguera, Montserrat Torné, Rubio, F. M., Fernandez, M., & J.L. García-Lobón. (2016). Updated Bouguer anomalies of the Iberian Peninsula: a new perspective to interpret the regional geology. *Journal of Maps*, 12(5), 1089–1092. <https://doi.org/10.1080/17445647.2015.1126538>
- Blakely, R. J. (1995). *Potential Theory in Gravity and Magnetic Applications*. <https://doi.org/10.1017/cbo9780511549816>
- Coiffier, G., Renard, P., & Lefebvre, S. (2020). 3D Geological Image Synthesis From 2D Examples Using Generative Adversarial Networks. *Frontiers in Water*, 2. <https://doi.org/10.3389/frwa.2020.560598>
- de la Varga, M., Schaaf, A., & Wellmann, F. (2019). GemPy 1.0: open-source stochastic geological modeling and inversion. *Geoscientific Model Development*, 12(1), 1–32. <https://doi.org/10.5194/gmd-12-1-2019>
- Dering, G. (2020). *Insights into dyke emplacement mechanisms using new high-resolution 3D digital outcrop methods*. <https://doi.org/10.26182/5eab97f21c63d>
- Fehler, M. C., & Keliher, P. J. (2011). *SEAM Phase I*. Society of Exploration Geophysicists.
- Garayt, C., Desassis, N., Samy Blusseau, Gibert, P.-M., Langanay, J., & Romary, T. (2025). Two-Dimensional Stochastic Structural Geomodeling with Deep Generative Adversarial Networks. *Mathematical Geosciences*, 57. <https://doi.org/10.1007/s11004-025-10188-3>
- Geoscience Australia. (2016). *Updated gravity datasets deliver a treasure map for mineral and energy exploration*. Ga.gov.au; c\=AU\;o\=Australian Government\;ou\=Geoscience Australia. <https://www.ga.gov.au/news/news-archive/updated-gravity-datasets-deliver-a-treasure-map-for-mineral-and-energy-exploration>
- Ghyselinck, S., Okhmak, V., Zampini, S., Turkiyyah, G., Keyes, D., & Haber, E. (2025). Synthetic Geology -- Structural Geology Meets Deep Learning. *ArXiv (Cornell University)*. <https://doi.org/10.48550/arxiv.2506.11164>
- Grudić, M., & Gurvich, A. (2021). pytreegrav: A fast Python gravity solver. *Journal of Open Source Software*, 6(68), 3675. <https://doi.org/10.21105/joss.03675>
- Grunnaleite, I., & Mosbron, A. (2019). On the Significance of Salt Modelling—Example from Modelling of Salt Tectonics, Temperature and Maturity Around Salt Structures in Southern North Sea. *Geosciences*, 9(9), 363. <https://doi.org/10.3390/geosciences9090363>

- Hajkowicz, S. A., Heyenga, S., & Moffat, K. (2011). The relationship between mining and socio-economic well-being in Australia's regions. *Resources Policy*, 36(1), 30–38.  
<https://doi.org/10.1016/j.resourpol.2010.08.007>
- Hector, B., & Hinderer, J. (2016). pyGrav, a Python-based program for handling and processing relative gravity data. *Computers & Geosciences*, 91, 90–97. <https://doi.org/10.1016/j.cageo.2016.03.010>
- Hudec, M. R., & Jackson, M. P. A. (2007). Terra infirma: Understanding salt tectonics. *Earth-Science Reviews*, 82(1-2), 1–28. <https://doi.org/10.1016/j.earscirev.2007.01.001>
- Intrepid Geophysics. (2021). *Home*. Intrepid Geophysics. <https://www.intrepid-geophysics.com/>
- Kavanagh, J. L. (2018). Mechanisms of Magma Transport in the Upper Crust—Dyking. *Volcanic and Igneous Plumbing Systems*, 55–88. <https://doi.org/10.1016/b978-0-12-809749-6.00003-0>
- Kernen, R., Amos, K. J., Anell, I., Evans, S., & Rodriguez-Blanco, L. (2024). The role of salt basins in the race to net zero: a focus on Australian basins and key research topics. *Australian Energy Producers Journal*, 64(2), S402–S406. <https://doi.org/10.1071/ep23213>
- Li, Y., Chen, S., Zhang, B., & Li, H. (2023). Fast imaging for the 3D density structures by machine learning approach. *Frontiers in Earth Science*, 10. <https://doi.org/10.3389/feart.2022.1028399>
- Li, Y., & Oldenburg, D. W. (1998). 3D inversion of gravity data. *GEOPHYSICS*, 63(1), 109–119.  
<https://doi.org/10.1190/1.1444302>
- M Lv, Zhang, Y., & Liu, S. (2023). Fast forward approximation and multitask inversion of gravity anomaly based on UNet3+. *Geophysical Journal International*, 234(2), 972–984.  
<https://doi.org/10.1093/gji/ggad106>
- M.B. Aminu, K.A.N. Adiat, A.A. Akinlalu, K.O. Olomo, Owolabi, T. O., & E.O. Aliyu. (2024). A review on the applications of airborne geophysical and remote sensing datasets in epithermal gold mineralisation mapping. *Geosystems and Geoenvironment*, 3(3), 100284–100284.  
<https://doi.org/10.1016/j.geogeo.2024.100284>
- Measham, T. G., Haslam Mckenzie, F., Moffat, K., & Franks, D. M. (2013). An expanded role for the mining sector in Australian society? *Rural Society*, 22(2), 184–194. <https://doi.org/10.5172/rsj.2013.22.2.184>
- Micklethwaite, S., Sheldon, H. A., & Baker, T. B. (2010). Active fault and shear processes and their implications for mineral deposit formation and discovery. *Journal of Structural Geology*, 32(2), 151–165.  
<https://doi.org/10.1016/j.jsg.2009.10.009>
- Misra, S., Chen, J., Churilova, P., & Falola, Y. (2024). Generative Artificial Intelligence for Geomodeling. *International Petroleum Technology Conference*. <https://doi.org/10.2523/iptc-23477-ms>
- N, N. M., E, A. M., Grauch, V. J. S, O, H. R., R, L. T., Li, Y., C, P. W., W, P. J., D, P. J., & E, R. M. (2005). Historical development of the gravity method in exploration. *GEOPHYSICS*, 70(6), 63ND89ND.  
<https://doi.org/10.1190/1.2133785>

- Nozaki, K. (2006). The generalized Bouguer anomaly. *Earth, Planets and Space*, 58(3), 287–303.  
<https://doi.org/10.1186/bf03351925>
- Rao, D. B. (1986). Modelling of sedimentary basins from gravity anomalies with variable density contrast. *Geophysical Journal International*, 84(1), 207–212.  
<https://doi.org/10.1111/j.1365-246x.1986.tb04353.x>
- Salehi, P., Abdolah Chalechale, & Taghizadeh, M. (2020). Generative Adversarial Networks (GANs): An Overview of Theoretical Model, Evaluation Metrics, and Recent Developments. *ArXiv (Cornell University)*. <https://doi.org/10.48550/arxiv.2005.13178>
- Scholz, C. (2007). The Scaling of Geological Faults. *11th International Conference on Fracture 2005, ICF11*, 8.  
<https://doi.org/10.1201/9780203936115.ch1>
- Talwani, M., Worzel, J. L., & Landisman, M. (1959). Rapid gravity computations for two-dimensional bodies with application to the Mendocino submarine fracture zone. *Journal of Geophysical Research*, 64(1), 49–59. <https://doi.org/10.1029/jz064i001p00049>
- Vladimir Puzyrev, Salles, T., Surma, G., & Elders, C. (2022). Geophysical model generation with generative adversarial networks. *Geoscience Letters*, 9(1). <https://doi.org/10.1186/s40562-022-00241-y>
- Wang, X., Chen, Y., & Zhu, W. (2021). A Survey on Curriculum Learning. *IEEE Transactions on Pattern Analysis and Machine Intelligence*, 1–1. <https://doi.org/10.1109/TPAMI.2021.3069908>
- Wellmann, F. (2022). Geological Modeling 4.0. *Springer EBooks*, 807–819.  
[https://doi.org/10.1007/978-3-662-64448-5\\_42](https://doi.org/10.1007/978-3-662-64448-5_42)
- Wigley, P. (2016). The development and evolution of the William Smith 1815 geological map from a digital perspective. *GSA Today*, 26(7), 4–10. <https://doi.org/10.1130/gsatg279a.1>
- Witter, J. B., Siler, D. L., Faulds, J. E., & Hinz, N. H. (2016). 3D geophysical inversion modeling of gravity data to test the 3D geologic model of the Bradys geothermal area, Nevada, USA. *Geothermal Energy*, 4(1). <https://doi.org/10.1186/s40517-016-0056-6>
- Wu, G., Wei, Y., Dong, S., Zhang, T., Yang, C., Qin, L., & Guan, Q. (2023). Improved Gravity Inversion Method Based on Deep Learning with Physical Constraint and Its Application to the Airborne Gravity Data in East Antarctica. *Remote Sensing*, 15(20), 4933–4933. <https://doi.org/10.3390/rs15204933>
- Zhou, S., Wei, Y., Lu, P., Yu, G., Wang, S., Jiao, J., Yu, P., & Zhao, J. (2024). A Deep Learning Gravity Inversion Method Based on a Self-Constrained Network and Its Application. *Remote Sensing*, 16(6), 995. <https://doi.org/10.3390/rs16060995>